tvst

Cornea & External Disease

A Biosynthetic Alternative to Human Amniotic Membrane for Use in Ocular Surface Surgery

Prity Sahay[1], Mehri Behbehani[2], Perla Filippini[1], Gianpaolo Bruti[2], Melissa Townsend[2], Rob McKean[2], and Harminder S. Dua[1]

[1] Academic Ophthalmology, Division of Clinical Neuroscience, School of Medicine, University of Nottingham, UK
[2] The Electrospinning Company, Oxfordshire, UK

Correspondence: Harminder S. Dua, Academic Ophthalmology, Division of Clinical Neuroscience, School of Medicine, University of Nottingham, Nottingham NG7 2RD, UK. e-mail: harminder.dua@nottingham.ac.uk

Received: December 18, 2023
Accepted: March 6, 2024
Published: May 2, 2024

Keywords: corneal reconstruction; synthetic amniotic membrane; human amniotic membrane; human corneal limbal epithelial cells; corneal surgical application

Citation: Sahay P, Behbehani M, Filippini P, Bruti G, Townsend M, McKean R, Dua HS. A biosynthetic alternative to human amniotic membrane for use in ocular surface surgery. Transl Vis Sci Technol. 2024;13(5):3, https://doi.org/10.1167/tvst.13.5.3

Purpose: The biosynthetic Symatix membrane (SM) was developed to replace fresh human amniotic membrane (hAM) in ocular surgical applications. The purpose of this study was to test the biocompatibility of the SM with human limbus–derived epithelial cells with regard to their physical and biological properties.

Methods: Different physical properties of SM were tested ex vivo by simulation on human corneas. In vitro, primary limbal epithelial cells from limbal explants were used to test biological properties such as cell migration, proliferation, metabolic activity, and limbal epithelial cell markers on the SM, hAM, and freeze-dried amniotic membrane (FDAM).

Results: The surgical handleability of the SM was equivalent to that of the hAM. Ultrastructural and histological studies demonstrated that epithelial cells on the SM had the typical tightly apposed, polygonal, corneal epithelial cell morphology. The epithelial cells were well stratified on the SM, unlike on the hAM and FDAM. Rapid wound healing occurred on the SM within 3 days. Immunofluorescence studies showed positive expression of CK-19, Col-1, laminin, ZO-1, FN, and p-63 on the SM, plastic, and FDAM compared to positive expression of ZO-1, Col-1, laminin, FN, and p63 and negative expression of CK-19 in the hAM.

Conclusions: These results indicate that the SM is a better substrate for limbal epithelial cell migration, proliferation, and tight junction formation. Altogether, the SM can provide a suitable alternative to the hAM for surgical application in sight-restoring operations.

Translational Relevance: The hAM, currently widely used in ocular surface surgery, has numerous variations and limitations. The biocompatibility of corneal epithelial cells with the SM demonstrated in this study suggests that it can be a viable substitute for the hAM.

Introduction

The first use of the human amniotic membrane (hAM) in ophthalmology was reported in the 1940s.[1] Since its reintroduction in 1995 to clinical practice and in the literature, it has been widely used with an expanding array of indications.[2,3] It does not, however, work equally for all indications. For some, such as persistent epithelial defects and reducing pain and inflammation in acute ocular surface inflammatory conditions as in Stevens–Johnson syndrome and chemical burns, it provides good outcomes.[4] For others, such as inhibiting vascularization and reducing scarring, the outcomes are equivocal, and failures have been reported.[5] One of the major limitations of the hAM is its manifold variations within and between donors and the risk of transmitting potentially lethal infectious diseases such as human immune deficiency virus and hepatitis B virus. Variations in thickness, transparency, cells lining the tissue, protein content, pro- and anti-inflammatory cytokines, and other molecules exist not only among donors but also within the same donor, depending on the site of the amniotic sac to the

placenta, age, parity, and whether or not the trial of labor was given. The multitude of processes involved in the handling, washing, freezing, or drying of the membrane further compound the variables.[6] The cost of storage and transportation (in dry ice for frozen membranes) is another limiting factor.

It is not surprising that the quest for a synthetic and standardized membrane that would obviate most if not all the above limitations is ongoing. The Electrospinning Company (Didcot, UK) has developed medical materials and products related to regenerative medicine based on electrospinning technology. One of the products is a biosynthetic degradable membrane made of electrospun poly(lactic-co-glycolic acid) (PLGA) and hyaluronan. PLGA is a synthetic and degradable polymer that, together with hyaluronan, has the potential to serve as a synthetic replacement for the hAM that can be used for multiple indications.[7] This membrane is a modified and improved version in terms of sterilization, long shelf-life, transparency, thickness, and shrinkage compared to the previous prototype.[8,9] Herein, we report the biocompatibility of the synthetic Symatix membrane (SM) with human corneal epithelial cells and its physical properties related to corneal surgical applications.

Methods

Surgical Assessment

By an optimization process related to the thickness, hyaluronic acid (HA) content, and alteration in membrane contour and size and stability in the culture medium, an "ideal membrane" was established by the evaluation of 30 different sets of synthetic membranes with different combinations of the above characteristics. The "ideal membrane" was determined to be the SM, which was used for all tests and experiments. Three sets of three SMs of 10-mm diameter from three different batches of production ($n = 9$ SMs) were tested for surgical and physical properties—namely, transparency, trephining, cutting, flexibility (draping on the cornea), suturing, and gluing. Each property was graded on a scale of 0 (not acceptable), 1 (average), 2 (good), 3 (very good), and 4 (excellent). Freeze-dried (lyophilized) amniotic membranes (FDAMs), sterilized by gamma irradiation (REGE pro gel; National Center for Radiation Research and Technology, Cairo, Egypt), and surgical-grade frozen hAMs were used as comparators.

SM discs of 10-mm diameter were removed from their sterile packing. The presence of static was documented by observing the distance the membrane moved from its original position in relation to the plastic container and cover of the packing. The details of physical properties and their methods of evaluation are listed below:

1. *Transparency*—SM discs were soaked in a balanced salt solution (BSS), and the transparency was graded before and after wetting.
2. *Trephination and cutting*—Both dry and wet SM discs were subjected to trephination (Barron Corneal Punch 7.5-mm; Corza Ophthalmology, Parsippany, NJ) and cutting with a pair of surgical scissors.
3. *Flexibility*—Wet membranes were draped on the surface of mounted human corneoscleral discs obtained from the eye bank on a Barron artificial anterior chamber (Corza Ophthalmology). The draping quality was assessed by the amount of "fish mouths" formed along the circumference.
4. *Suturing*—Each SM disc was then sutured on the cornea with 8-bite running 10-0 nylon monofilament suture with a side cutting needle (nylon, black monofilament, non-absorbable suture; Alcon Laboratories, Fort Worth, TX). The size of the needle hole in the SM and any cheese-wiring of the suture in the SM were noted. The corneoscleral discs with the sutured SMs were dismounted, placed in a six-well tissue culture plate, and submerged in a growth medium containing Dulbecco's Modified Eagle's Medium (DMEM) supplemented with 10% fetal bovine serum (FBS) and 1× penicillin–streptomycin for 3 weeks. Photographs were taken with a stereomicroscope (Leica S6 D; Leica Microsystems, Wetzlar, Germany) at baseline and twice every week to evaluate the physical state of the SMs (size, shape, and state of sutures and suture holes). A control SM disc was placed in the medium alone for the corresponding duration.
5. *Gluing*—Fibrin glue (Tisseel; Baxter Healthcare, Deerfield, IL) was used for the gluing SMs on different sets of mounted corneoscleral discs from which the epithelium was removed. The thin component of glue (human thrombin, 500 IU/mL) and calcium chloride (40 µmol/mL) was applied to the surface of the cornea and the thick component (human fibrinogen, 72–110 mg/mL, and aprotinin, 3000 KIU/mL) to dry SMs. The latter were then turned over and placed on the cornea to allow the two components to mix. The SM was gently pressed on the corneal surface with a surgical sponge and allowed to sit for

Table 1. Physical Properties of the SM Compared to the FDAM and hAM

Physical Property	SM	FDAM	hAM
Flexibility	3	4	4
Transparency	1	2.5	3
Cutting	4	3	3
Trephining	4	3	3
Suturing	3	4	4
Gluing	2.5	3	4

Scoring system: 0, not acceptable; 1, average; 2, good; 3, very good; 4, excellent.

5 minutes. The SM was then peeled off by the surgeon and the firmness of adhesion was subjectively evaluated and the ease of these objectives was assessed and graded (Table 1).

Establishment and Maintenance of Human Limbal Epithelial Cell Culture

Residual corneoscleral rims after corneal transplantation were obtained from donor eyes less than 80 years of age ($n = 3$). The tissues were obtained from the National Health Service-Blood and Transplant service and the experiments were carried out in the Larry A. Donoso Eye Research Laboratory, the University of Nottingham, and the Nottingham University Hospital NHS Trust. The use of human corneal rims post-transplantation was covered under the Human Tissue Act Licence (HTA-12265). The SMs, FDAMs, and hAMs were affixed in a plastic scaffolding (15 mm; Scaffdex, Tampere, Finland) to keep the membranes taut and were then placed in 12-well tissue culture plates. Limbal epithelial cell cultures were obtained from residual corneoscleral rims after corneal transplantation within 3 to 4 weeks of retrieval and 24 hours of the operation. The Descemet's membrane with endothelial cells was removed and discarded. The corneoscleral rim was washed three times with 1× Dulbecco's phosphate-buffered saline (DPBS) containing antibiotics to generate explant cultures of limbal epithelium. After careful removal of the excessive sclera, the trabecular meshwork, and any remnants of iris under a stereomicroscope, the rims were cut into smaller pieces of about 2 mm × 2 mm. They were then explanted directly onto six-well (35-mm) tissue culture plates for human limbal epithelial cells (hLEC) culture on the three different membranes (for morphological study and immunofluorescence [IF]) or onto 13-mm round glass coverslips (for IF). The limbal explants were incubated for 30 minutes to promote adhesion to the substrate. Thereafter, the cultures were maintained in a growth medium of DMEM/Nutrient Mixture F-12 (1:1) containing Gibco GlutaMAX (Thermo Fisher Scientific, Waltham, MA), 10% FBS, and 1% penicillin–streptomycin at 37°C. The medium was changed on alternate days, and the extent of outgrowth was monitored with an inverted microscope (Eclipse TS100; Niko, Tokyo, Japan). After 4 weeks, when explants in the six-well culture plates reached confluency, the cells were harvested by trypsinization with 0.25% trypsin/ethylenediaminetetraacetic acid (EDTA) at 37°C for 5 minutes. The cell suspension was centrifuged at 1200 rpm for 5 minutes and seeded in a T-25 tissue culture flask. Passage 2 and passage 3 cells were used for the experiments described below.

Scanning Electron Microscopy

The epithelial cells grown on the SMs were initially fixed in 3% glutaraldehyde for at least 30 minutes at room temperature (RT) and then washed three times 0.1-M phosphate/cacodylate. Samples were post-fixed for at least 30 minutes at RT in 1% osmium tetroxide (OsO_4), and then dehydrated in a graded series of ethanol. The final dehydration was performed using the Critical Point Dryer (Leica Microsystems) following mounting on coated carbon stubs (sputtered) with platinum (10-nm thickness). Coated preparations were observed and photographed with scanning electron microscopy (SEM; Philips XL-30 SEM; Philips, Amsterdam, Netherlands).

Stratification With Air-Lifting

The hLECs were grown on SMs, FDAMs, and hAMs. Two different groups of cultures were established: air-lifting (AL) and non–air-lifting (non-AL). The non-AL cultures were continuously submerged in the growth medium for 18 days. The AL cultures were first submerged in the medium until they reached confluency (4 days) and then exposed to air by lowering the level of the medium for 14 days. On alternate days, the medium was changed and the surface was washed with 1× DPBS to remove accumulated debris. The lowering of the medium was adjusted to keep the surface moist.

Proliferation, Migration, and Metabolic Assay

An equal density of hLECs was seeded on SMs, FDAMs, and hAMs contained in 12-well plates. Cells seeded directly on the bottom of 12-well plates (plastic) or coverslips served as controls. The proliferation assay was performed by Ki-67 staining at days 1, 3, and 6 of the experiment. The number of Ki-67–positive epithe-

Table 2. Abcam Antibodies Used in This Study

Antibodies	Catalog No.	Source	Clonality	Dilution
Cytokeratin-3 (CK-3)	ab77869	Mouse	M	1:200
Cytokeratin-19 (CK-19)	ab76539	Rabbit	M	1:200
p63	ab124762	Rabbit	M	1:200
Fibronectin (FN)	ab2413	Rabbit	P	1:100
Zonula occludens-1 (ZO-1)	ab216880	Rabbit	P	1:100
Ki-67	ab16667	Rabbit	M	1:250
Collagen I (Col-1)	ab138492	Rabbit	M	1:500
Laminin	ab11575	Rabbit	P	1:50
Phalloidin	ab176757	NA	NA	1000×
Anti-rabbit Alexa Fluor 488	ab150081	Goat	P	1:1000
Anti-mouse Alexa Fluor 488	ab150117	Goat	P	1:1000

M, monoclonal; P, polyclonal.

lial cells was counted, and the ratio of proliferating to total cells was calculated. Five different locations at 10× were counted for each sample.

For the migration assay, when the cells reached confluency, a scratch wound was created with a 200-µL tip. The wounds were monitored for 24, 48, and 72 hours under an inverted microscope (DM IL LED Fluo; Leica Microsystems), and images were captured to visualize the closure of the wounds between the edges of the scratched areas. At each time point, the cells on the SMs, FDAMs, and hAMs were stained with hematoxylin and eosin (H&E) to visualize and record the progress of wound closure by light microscopy (DM 1000 LED; Leica Microsystems).

A resazurin assay was performed to determine the metabolic activity of the cells seeded on the SMs, FDAMs, hAMs, and plastic controls. An equal density of hLECs was seeded on each membrane. The experiment was performed based on the manufacturer's protocol (ab129732; Abcam, Cambridge, UK). The metabolic activity was assessed at 1, 3, and 6 days of the experiment. The fluorescence intensity was measured at 590 nm using a 540-nm excitation wavelength with a microplate reader (CLARIOstar; BMG Labtech, Ortenberg, Germany). The data were analyzed using R-Studio 5.40 (R Foundation for Statistical Computing, Vienna, Austria). Assays were run in triplicate with three independent experiments. Prism 10 (GraphPad, Boston, MA) was used to plot a graph to compare the metabolic activity of cells on each membrane.

Immunofluorescence

To examine the cellular properties of corneal limbal epithelial cells, we checked such markers as conjunctival and limbal epithelial cells, including cytokeratin-19 (CK-19); cell differentiation epithelium, cytokeratin-3 (CK-3); cell-extracellular matrix attachment protein, fibronectin (FN); basement membrane and adhesion protein (laminin); tight junction protein, zonula occludens-1 (ZO-1); the most abundant collagen in the cornea, collagen-1 (Col-1); and the stem cell marker p63 in the plastic controls, SMs, FDAMs, and hAMs. Whole-mount membranes were stained by respective monoclonal/polyclonal antibodies (Table 2) with the double-labeled phalloidin for F-actin and cell nuclei with 4′,6-diamidino-2-phenylindole (DAPI). Briefly, an equal density of hLECs was seeded on the SMs, FDAMs, hAMs, and coverslip as control. To examine p63 in the primary outgrowth limbal epithelial cells, limbus explant was put directly on the coverslip and the membranes. On the day of staining, the cells on the membranes and coverslip were fixed with 4% paraformaldehyde (PFA) for 20 minutes and permeabilized with 0.1% Triton X-100 in PBS for 15 minutes at RT. The samples were blocked with 10% normal goat serum for 1 hour at RT and sequentially incubated overnight at 4°C with specific primary monoclonal or polyclonal antibodies at appropriate dilutions (Table 2) in 5% normal goat serum. Each section was washed three times with PBS and incubated with respective fluorescent dye-conjugated secondary antibodies at appropriate dilutions (Table 2) in 5% normal goat serum for 1 hour in the dark at RT. After three washes with 1× PBS for 5 minutes each, the sections were mounted on a coverslip with DAPI containing mounting medium (Invitrogen ProLong Diamond Antifade Mountant with DAPI; Thermo Fisher Scientific). The samples were imaged using a fluorescent microscope (DMIL LED Fluo; Leica Microsystem) and confo-

cal microscopy (LSM880C; Carl Zeiss Microscopy, Oberkochen, Germany). The images were analyzed using Leica Application Suite X (3.0.0.15697) and Zen 2.1 SP3 software.

Results

Ex Vivo Assessment of Surgical Handleability of the SMs

The dry SMs demonstrated some static on opening the packing, but the static was lost upon wetting. The SMs were opaque (white) when dry but became translucent with wetting. The overall transparency of the SMs was less than that of the FDAMs and hAMs. Other physical characteristics such as cutting and trephining on dry and wet SMs were similar to those of the FDAMs and hAMs. However, unlike the FDAMs and hAMs, the SMs were not as flexible and did not drape the cornea perfectly. Three or four prominent folds, like fish mouths, were seen along the circumference (Fig. 1A). Nonetheless, suturing the wet SM to the cornea was as good as for the FDAMs and hAMs, and the fish mouths flattened considerably. The passage of the needle and suture through the SMs was easy and did not result in tearing of the membrane or breakage of the sutures. After the sutured SMs were submerged in medium, a slight enlargement of the holes created by the needle passes was seen in the first week but remained stable thereafter. The SMs retained their shape and size in the culture medium until 15 to 18 days, but the surface area enlarged around day 19 and remained so until the conclusion of the experiment (23 days) (Fig. 1A). The adhesive effect of fibrin glue on the denuded corneal surface was similar between the SM and FDAM but less than with the hAM (data not shown for FDAM and hAM) (Fig. 1B, Table 1).

In Vitro Testing of Biological Compatibility of SM With hLECs

SM Epithelial Morphology and Phenotype for the Limbal Explant Culture System

The rate of epithelial outgrowth from the plastic and SM explants was slow for the first week but rapidly increased to a size of 2 to 3 cm in diameter by 2 to 3 weeks, comparable to the FDAMs and hAMs. The cells on the FDAMs and hAMs were examined by staining the nucleus with DAPI, and actin filaments with phalloidin using the IF assay. The epithelial cells of the hLEC outgrowth exhibited similar morphology to the corneal epithelium, including a cohesive sheet of uniformly small, polygonal, and compact basal epithelial cells with a nucleus-to-cytoplasm ratio of close to 1:1. The cell outgrowth reached confluence by 3 weeks (Fig. 2).

Examination of the apical surface of the cultured limbus-derived epithelial cells by SEM on the SM showed a continuous layer of flat polygonal epithelial cells (Fig. 3B). The cells were similar in appearance to normal corneal epithelial cells. The cultivated cells were closely attached to each other with cell junctions and distinct cell boundaries (Fig. 3C). The epithelial cells at the edge of the sheet showed lamellipodia extending on the SM (Fig. 3D).

SM Stratification and Differentiation of Cultured Cells With Air-Lifting

Evaluation of hLECs on the SM, plastic, FDAM, and hAM by AL and non-AL techniques revealed that the cells on the SMs had stratified by 2 weeks of AL. The epithelial cells showed two or three cell layers of stratification, and the corneal cell differentiation was confirmed by the expression of CK-3 in the stratified epithelium on SM. No CK-3 expression was detected in non-AL cells. The epithe-

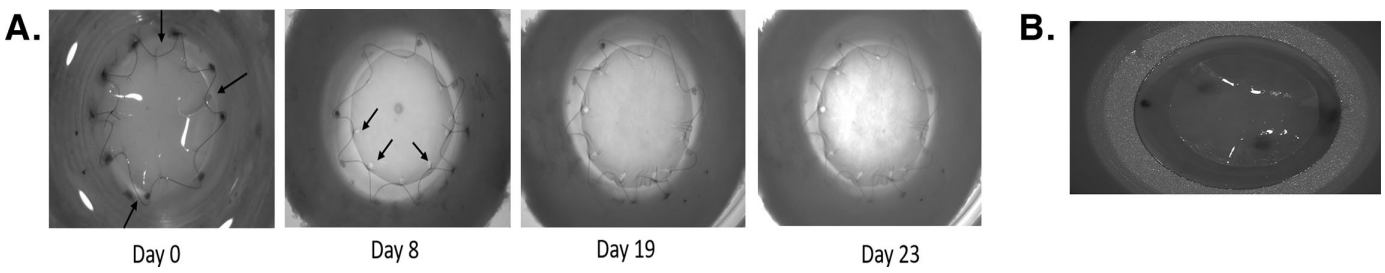

Figure 1. Surgical handleability of the Symatix membrane. (**A**) SM sutured to the corneoscleral disc and maintained in the medium for 23 days. Minor enlargement of the holes was seen on day 8 but no tearing of the membrane or breakage of the sutures was seen until the conclusion of the experiment (day 23). *Arrows* point to the fish mouthing observed. (**B**) Gluing the SM to the corneoscleral disc with biological fibrin glue.

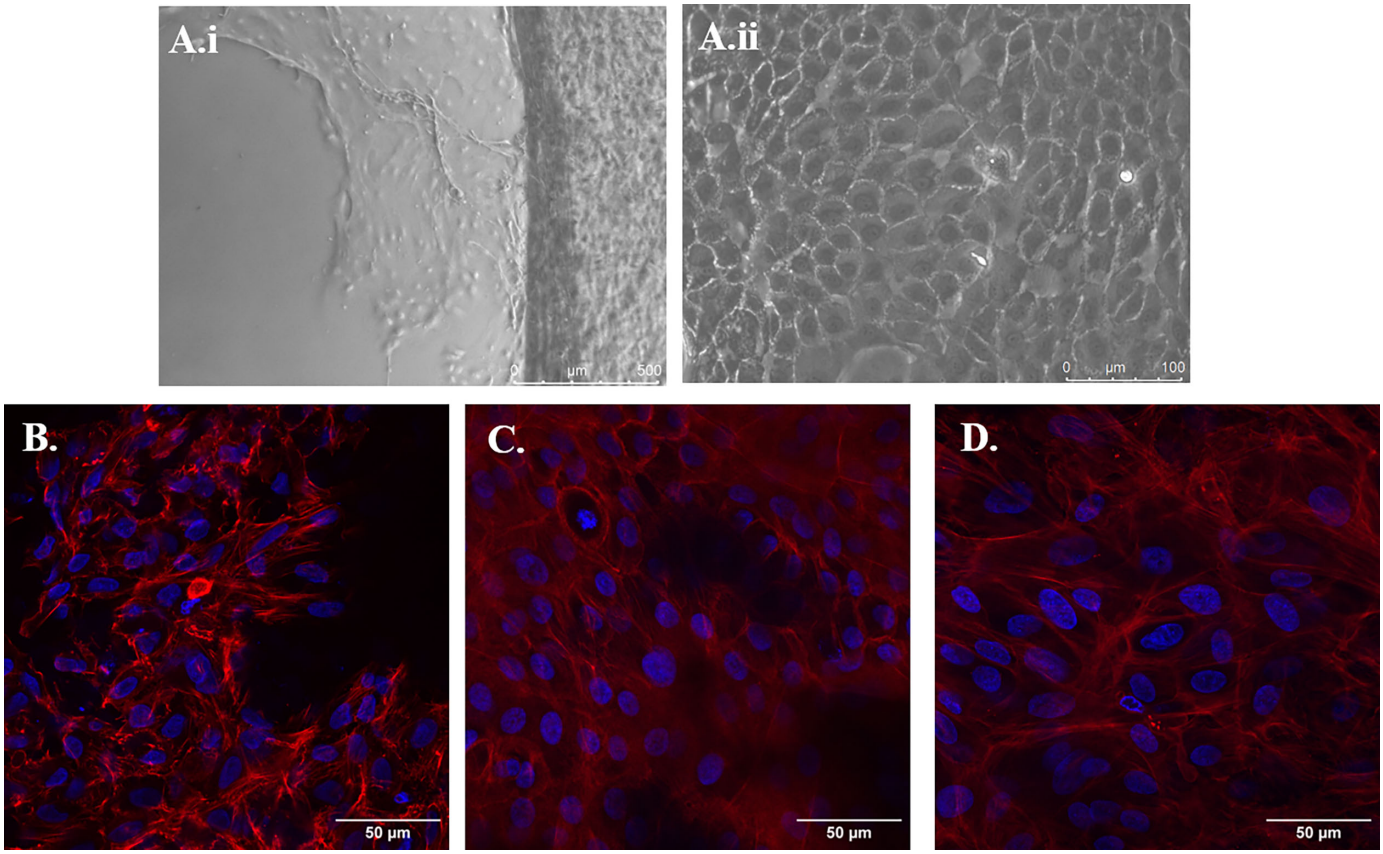

Figure 2. Epithelial cell morphology and phenotype on plastic, SMs, FDAMs, and hAMs of the limbal explant cultures. (**A.i**) Explant growth on plastic after 3 days. *Scale bar*: 500 µM. (**A.ii**) Explant growth on plastic after 2 weeks. *Scale bar*: 100 µM. Image was taken with a brightfield microscope. (**B**) Explant growth on SM after 2 weeks. *Scale bar*: 50 µM. (**C**) Explant growth on the FDAM after 2 weeks. *Scale bar*: 50 µM. (**D**) Explant growth on the hAM after 2 weeks. *Scale bar*: 50 µM. Images were taken by confocal microscopy. *Red* indicates actin filaments, and *blue* indicates DAPI/nuclear staining. Magnification: 5× (*scale bar*: 500 µM), 20× (*scale bar*: 100 µM), and 40× (*scale bar*: 50 µM).

lial cells in FDAM, both AL and non-AL, had not stratified and did not show CK-3 expression (Fig. 4).

SMs Promote Proliferation, Migration, and Metabolic Activity of Epithelial Cells

As indicated by Ki-67 staining, the proliferation assay demonstrated that Ki-67–positive cells increased in number up to 3 days (approximately 60% confluence) but significantly decreased by the sixth day (100% confluence). This trend was seen in cells cultured on plastic, SMs, FDAMs, and hAMs (Figs. 5A, 5B). The scratch assay demonstrated rapid healing on the SM, in 3 days, similar to that on plastic (Fig. 5C). The scratch assay was difficult to perform on the FDAM or hAM without damaging the underlying tissue. Moreover, the cell sheets were not as confluent on the FDAM and hAM; hence, conclusive data on wound closure were not obtained (Supplementary Fig. S1). Assay of metabolic activity by the resazurin assay showed a similar trend with increasing metabolic activity up to 3 days and a decline thereafter on day 6 on the plastic, SM, FDAM, and hAM, the same as the proliferation assay (Fig. 5D).

Expression of Limbal Epithelium, Tight Junction, and Stem Cell Markers on SM

The IF study showed positive expression of CK-19, FN, laminin, and Col-1 on plastic, SM, and FDAM compared to positive expression of FN, laminin, and Col-1 and negative expression of CK-19 on hAMs in the cultured cells (Fig. 6A). ZO-1 expression in cell boundaries in a pattern consistent with the formation of typical junctional complexes was found in the SM, plastic, and FDAM compared to lower expression on the hAM (Fig. 6B). However, the expression of p63 was high in the nuclei of the epithelial cells grown on the SM, FDAM, and hAM compared to plastic in an explant cultured system (Fig. 7).

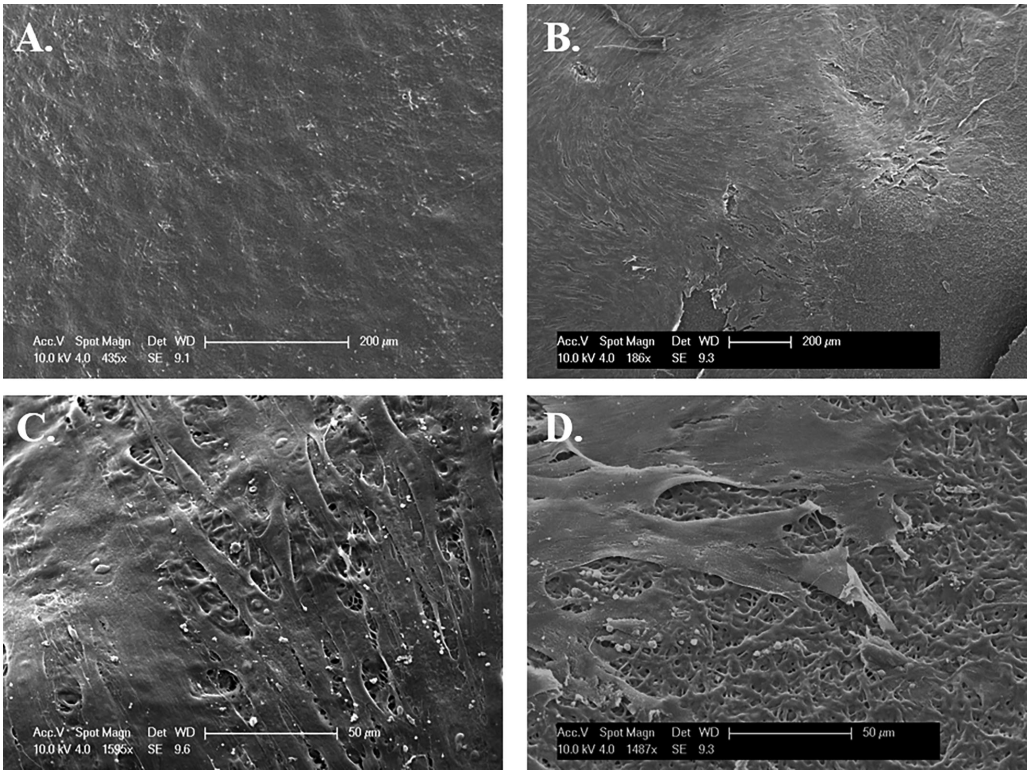

Figure 3. SEMs of human limbus-derived epithelial cells cultured on SMs. (**A**) SM with no cells; (**B**) Epithelial cells are closely attached to each other with tightly opposed cell–cell junctions. (**C**) Epithelial cells with distinct cell borders on the SM. (**D**) Epithelial cells at the edge of the sheet showing lamellipodia extending on the SM.

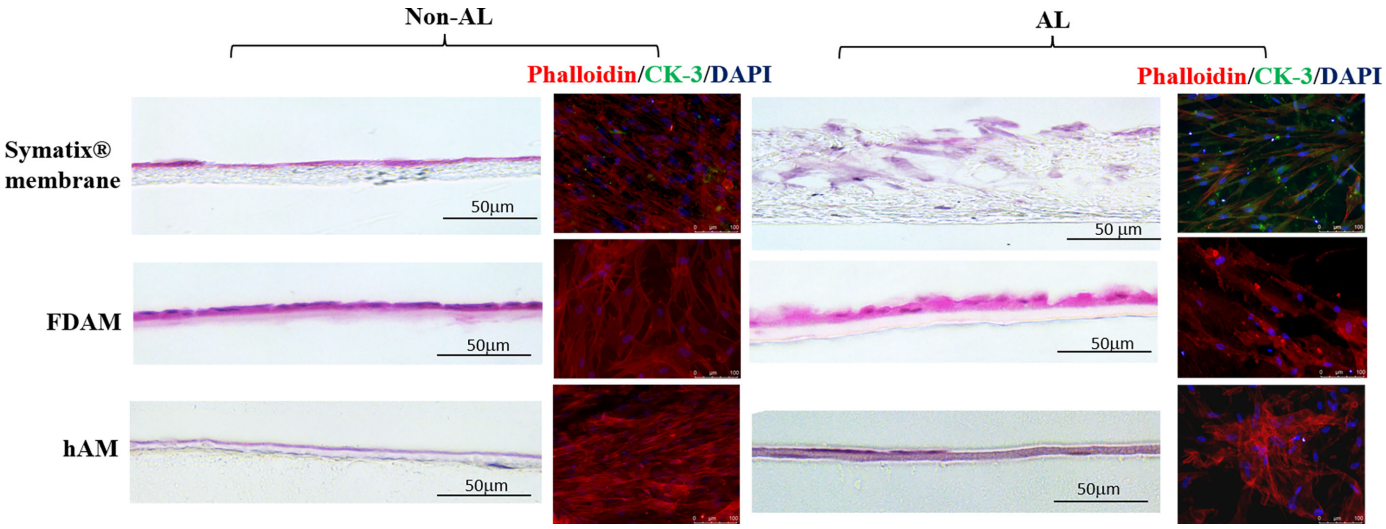

Figure 4. Stratification and differentiation of cultured epithelial cells on the SMs, FDAMs, and hAMs with and without air-lifting for 2 weeks. (*Left panel*) Membranes without air-lifting (non-AL). H&E staining of the cryosections shows the cells on the top of the membranes. No stratification was seen on the cells without air-lifting after 2 weeks. CK-3 (*green*)–negative cells were seen on whole-mount staining of the membranes by IF assay. (*Right panel*) Membranes with air-lifting (AL). The epithelial cells on SM showed two or three cell layers of stratification by H&E staining after air-lifting for 2 weeks. CK-3 (*green*)–positive cells were seen on whole-mount staining of the SMs by IF assay. No stratification and CK-3 positive cells were observed on the FDAMs or hAMs. *Red* indicates actin filaments, and blue indicates DAPI/nuclear staining. Magnification: 10× (*scale bar*: 100 µM) and 40× (*scale bar*: 50 µM).

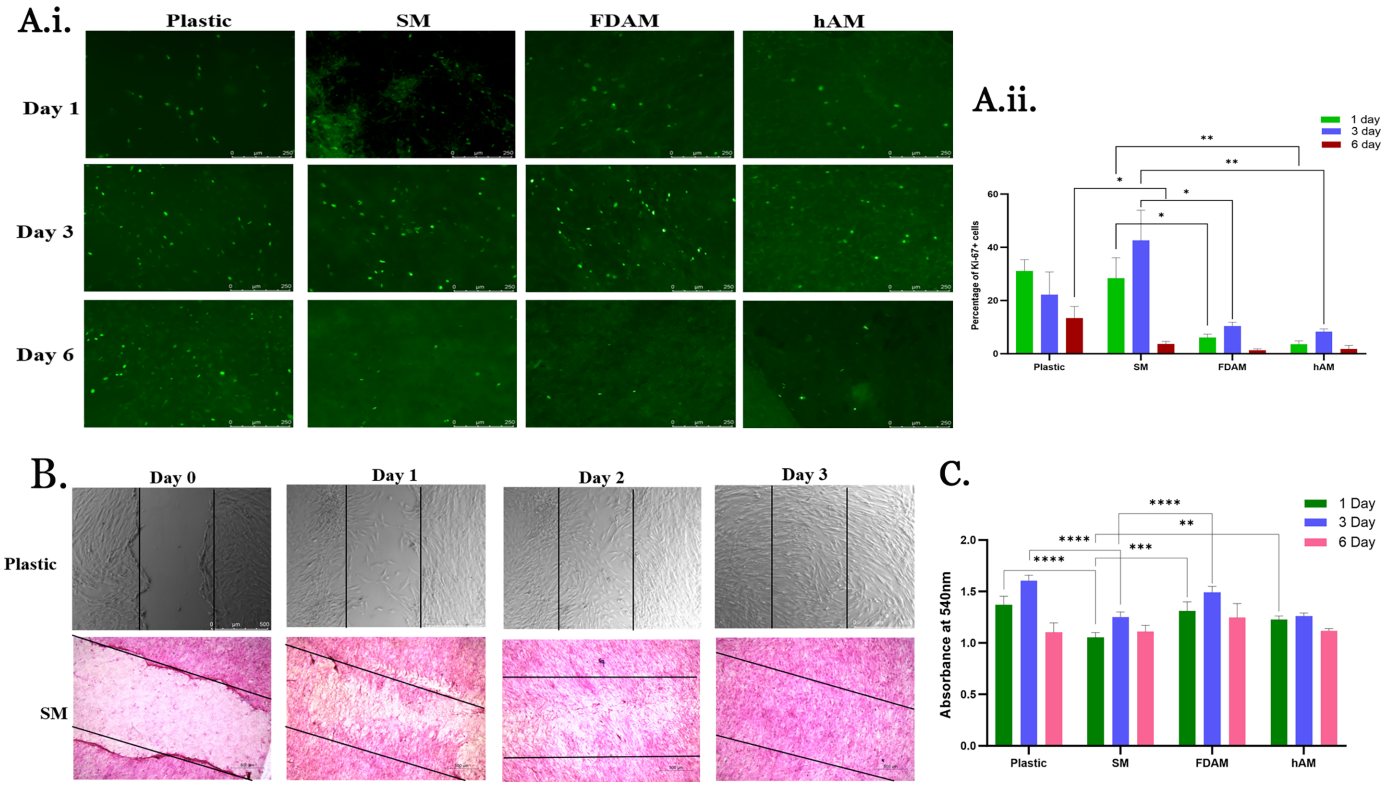

Figure 5. Proliferation, migration, and metabolic activity of epithelial cells on the SMs, FDAMs, and hAMs. (**A.i**) Ki-67 (*green*) staining on the plastic, SMs, FDAMs, and hAMs for days 1, 3, and 6. *Scale bar*: 25 µM). Increasing proliferation was observed from days 1 to 3 and then declining proliferation on day 6 on the plastic, SMs, FDAMs, and hAMs. (**A.ii**) A graph showing the percentage of Ki-67–positive cells on all the membranes. (**B**) Scratch assay on the plastic and SM by H&E staining. *Scale bar*: 500 µM. Rapid healing was seen on the SM, as seen on plastic, in 3 days. (**C**) Graph shows metabolic activity by the resazurin assay; the metabolic activity increased from days 1 to 3 and then declined on day 6 on all the different substrates. Means ± SD are shown. *$P < 0.05$, **$P < 0.01$, ***$P < 0.001$, and ****$P < 0.0001$ (two-way ANOVA with Tukey multiple comparison test). Magnification: 5× (*scale bar*: 500 µM) and 10× (*scale bar*: 250 µM).

Discussion

The human amniotic membrane is used extensively for a wide range of clinical indications but specifically for conditions affecting the eye such as non-healing corneal epithelial defects.[5,10–12] The membrane is used as a graft (inlay) to fill a corneal melt or as a sheet on which the epithelial cells grow and incorporate the amnion in the corneal tissue. It is often used as a patch (onlay) to provide cover for a finite period, after which it falls off or is removed.

Clinical experience has shown that the application of the membrane to the eye is not always successful, and failures have been reported,[13–15] which could be related to the various limitations of the membrane. Numerous intra- and inter-donor differences have been noted with regard to membrane thickness, transparency, epithelial cell morphology,[16] growth factor distribution and concentration,[17–19] race,[20] gravidity and parity,[21] and the onset of labor or not[22,23] of the donors. The role of growth factors and other proteins in hAMs is inconclusive, especially because the concentration and activity in the stored (frozen or dried) membrane are unknown or at best variable. There is no doubt, however, that the membrane provides a substrate allowing the cells to grow, migrate, and attach.[3,24]

The environmental and financial impact of storing and transporting frozen membranes is well recognized. "Dried" membranes have been developed that can be stored at room temperature and are easy to transport but all of the above limitations remain. The risk of transmission of infectious diseases is of concern. Though strict measures are in place in developed countries, they are not common practice in other parts of the world. Gamma irradiation can be used to sterilize hAMs but causes structural changes to the membrane leading to a significant decrease in several growth factors.[25,26]

The quest for a synthetic, standard membrane that is free from all the aforementioned limitations has

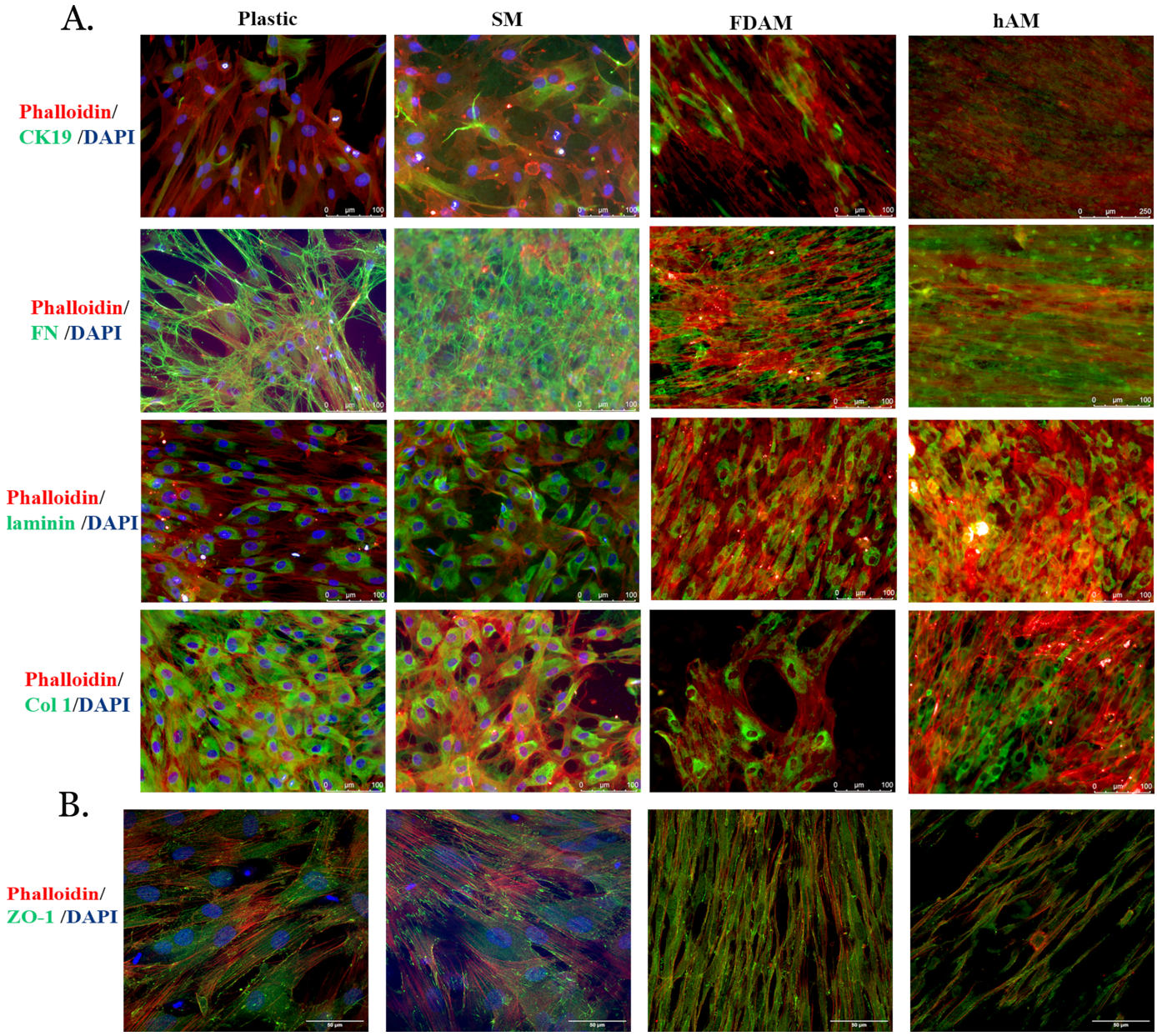

Figure 6. Localizations and expression of cell markers and tight junction protein in cultured limbal epithelial cells on the plastic, SMs, FDAMs, and hAMs. (**A**) *Row 1* shows CK-19 (*green*) expression that was seen in the cytoplasm of corneal-specific epithelial cells on the plastic, SMs, and FDAMs but not on the hAMs. *Scale bar*: 100 µM. *Row 2* shows the FN (*green*) expression seen on the extracellular matrix indicating attachment and spreading of epithelial cells on the plastic, SMs, FDAMs, and hAMs . *Scale bar*: 100 µM. Row 3 shows laminin (*green*) expression seen in cytoplasm and actin filaments indicating adhesion, migration, and proliferation of epithelial cells on the plastic, SMs, FDAMs, and hAMs. *Scale bar*: 100 µM. *Row 4* shows Col-1 (*green*) expression seen on the epithelial cells by fluorescence microscope indicating the most abundant collagen present in the limbus-derived epithelial cells on the plastic, SMs, FDAMs, and hAMs. *Scale bar*: 100 µM. (**B**) Expression of ZO-1 was seen on actin filaments and cytoplasm, illustrating integral transmembrane tight junction protein in limbus-derived epithelial cells by confocal microscope. *Scale bar*: 50 µM. *Red* indicates actin filaments, and *blue* indicates DAPI/nuclear stain. Magnification: 20× (*scale bar*: 100 µM) and 40× (*scale bar*: 50 µM).

remained the holy grail. The SM, which is an electrospun synthetic membrane impregnated with sodium hyaluronate, is devoid of all of the above limitations and offers the advantages of consistency in content and thickness. Its transparency is clinically acceptable, being as good as the hAM but less than the FDAM. Its comparative stiffness makes it easier to handle and manipulate surgically with forceps, scissors, and trephines. It can be glued and/or sutured on the human cornea without the sutures cutting through. With fibrin

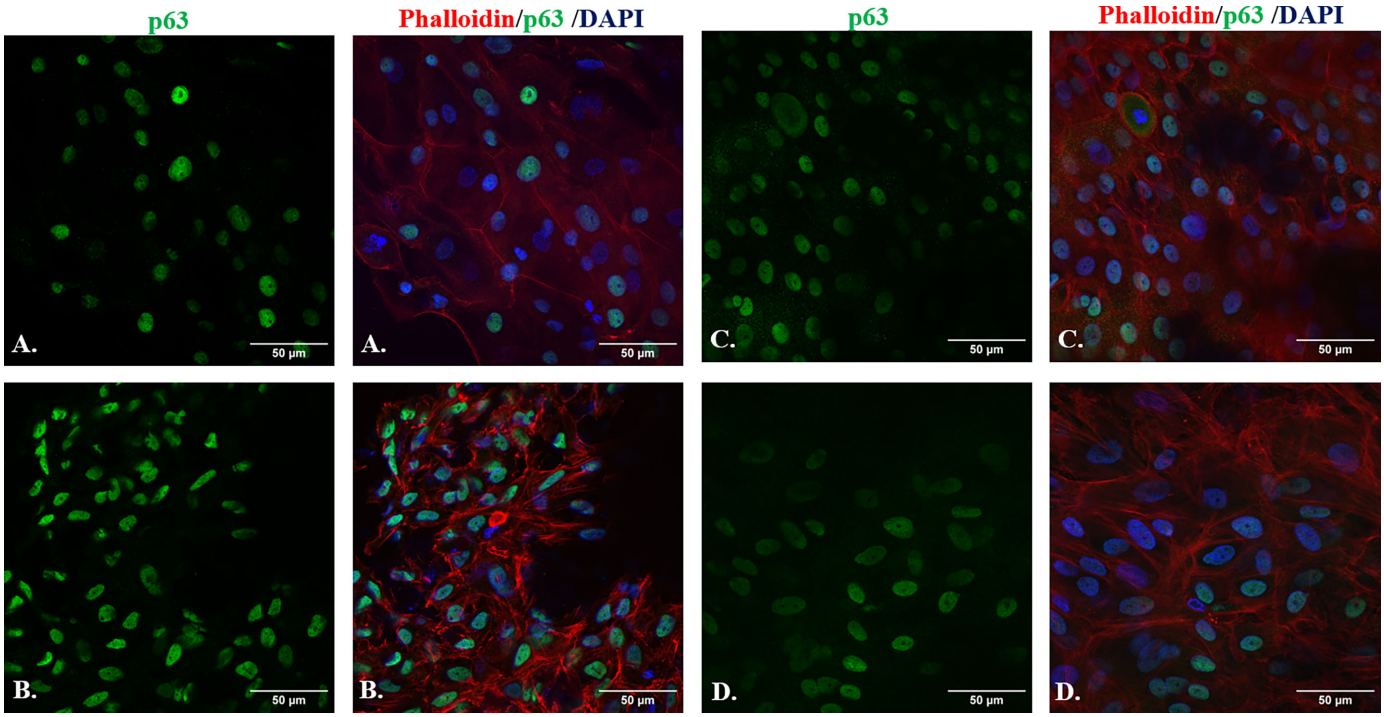

Figure 7. Localization and expression of stem cell marker (p63) on explant cultured epithelial cells on the plastic, SMs, FDAMs, and hAMs. Expression of p63 (*green*) was seen in the nucleus of limbal explant (limbus)–derived and cultured limbus-derived epithelial cells indicating the presence of stem cells in the group of epithelial cells on plastic (**A**), SMs (**B**), FDAMs (**C**), and hAMs (**D**) by confocal microscope. *Scale bar*: 50 µM. Increased p63-positive cells were present in all three membranes (**B**–**D**), unlike decreased p63-positive cells on the plastic controls (**A**). *Red* indicates actin filaments, and *blue* indicates DAPI/nuclear stain. Magnification: 40×. *Scale bar*: 50 µM.

glue, the adhesion was as good as that of the FDAM but not as good as for the hAM. This is likely to be related to the presence of the spongy layer in the hAM, which soaks the glue better. The spongy layer is absent in the FDAM and SM.

In vitro, biocompatibility with human corneal epithelial cells was shown to be very good. Limbus-derived corneal epithelial cells, placed on the SM directly from cell cultures or derived from limbal explants placed on the SM, showed cell migration, adhesion, and stratification similar to that with the FDAM and hAM. The study demonstrates that hLECs can expand on the SM using the limbus explant system, which is more akin to the clinical situation where the membrane would be used as a substrate for limbus-derived cells to grow and cover a non-healing epithelial defect. Moreover, filopodia and lamellipodia extending from cells at the edge of a migrating sheet on the SM, as seen by SEM, indicated a normal pattern of behavior of migrating corneal epithelial cells. Epithelial cell stratification was readily achieved on the SM, indicating that the same is likely to occur in vivo, as would be desired.[27]

By air-lifting, stratification and differentiation were achieved on the SM but not on the FDAM or hAM. Similar studies on denuded and intact hAMs have shown that stratification of epithelial cells was only achieved on denuded AMs but not on intact AMs.[28] Expression of CK-3 on the superficial cells of the stratified sheet on the SM suggests that the cells were maturing into terminally differentiated corneal epithelial cells. CK-19 and CK-3 have been extensively used as cornea-specific epithelial markers.[29,30] We noted a positive expression of CK-19 protein and a negative expression of CK-3 in all SMs and FDAMs (data not shown) compared with plastic in early cultures of limbal epithelial cells. Surprisingly, the expression of CK-19 is absent in hAMs; however, positive expression of CK-3 occurred after 2 weeks of air-lifting. Such an expression pattern has been reported in the corneal epithelium in a three-dimensional–limbal explant culture model, which showed positive staining for CK-19 and negative expression of CK-3 in early cultures.[31]

The scratch test assay for wound healing was very favorable for the SM, with wounds healing in 3 days, compared to the rates of healing for the FDAM and hAM (see Supplementary Fig. S1). The proliferation and metabolic activity studied by Ki-67 staining and resazurin assay, respectively, peaked at 3 days and declined by day 6 on all substrates studied. As cells had

attained 100% confluence by day 6, it is likely that the migration activity and correspondingly the metabolic activity too declined.

It is known that laminin, FN, and Col-1 promote corneal epithelial cell adhesion and increase the motility of corneal epithelial cells.[32] FN has a major function in inducing membrane protrusion or lamellipodia in the direction of cell movement. Furthermore, FN also induces the accumulation of a thick rim of F-actin and the formation of large focal adhesions at the periphery of corneal epithelial cells. Col-1, Col-4, and laminin support the formation of a thin rim of F-actin at the cell periphery and the formation of focal adhesions. Altogether, these proteins play a major function in the adhesion, motility, and morphology of epithelial cells.[32] Our study showed positive expression of laminin, FN, and Col-1 in all three membranes, indicating increasing cell adhesion and motility of corneal epithelial cells.

Epithelial tight junctions consist of integral transmembrane proteins such as claudin and occludin, membrane-associated proteins (including ZO-1, -2, and -3), and actin filaments, and they subserve the barrier function of epithelia.[33,34] ZO-1 is expressed in superficial and subsuperficial cell layers of the corneal epithelium and contributes to the barrier function of this epithelium.[35] Epithelial cells on the SM and other membranes showed ZO-1 expression, indicating the formation of tight junctions. Increased intensity of ZO-1 in subsuperficial cells suggests that ZO-1 within the corneal epithelium cells may be exclusively associated with not only the formation of tight junctions but also the establishment of a barrier to paracellular flow and in the cell–cell adhesion of basal and wing epithelial cells and the anchorage of the adhesion complexes to the actin cytoskeleton. To demonstrate and study the ultrastructure of the adhering junctions such as hemidesmosomes and desmosomes, we tried transmission electron microscopy (TEM) of the cell sheets on SMs. Unfortunately, the SMs completely dissolved in the last step of dehydration with 100% propylene oxide and TEM could not be carried out.

The p63 molecule has been proposed to be a marker for stem cells in the limbus, corneal, and conjunctival epithelial cells.[36–38] Expression of p63 was substantial and comparable in all three membranes, unlike in the plastic controls where it was much lower. This indicates that the SM supports stem cells like the amniotic membrane.

Our study thus demonstrates that the SM has the potential to be a suitable biosynthetic alternative to hAM in corneal and ocular surface surgery. It offers the advantages of uniform thickness, which can be tailored; consistency in content; and ease of sterilization, storage, transport, and surgical application with no risk of transmission of bloodborne infections, and it obviates all the variations seen with human amnion. Studies to evaluate its safety and efficacy in vivo, where its biodegradability will also be assessed in a phase 1 clinical trial, are planned and are under consideration of regulatory authorities.

Acknowledgments

The authors thank Lorelei Robertson and Martin Roe from Nanoscale and Microscale Research Centre, the University of Nottingham, for their participation in the SEM.

Supported by a United Kingdom Research and Innovation grant (project ID-5048175).

Disclosure: **P. Sahay**, None; **M. Behbehani**, None; **P. Filippini**, None; **G. Bruti**, None; **M. Townsend**, None; **R. McKean**, None; **H.S. Dua**, Artic Vision (C, R, S), Thea Pharmaceuticals (C, R), Seagen (R), Electrospinning Company (F, R), NuVision Biotherapies (I, P), GlaxoSmithKline (I)

References

1. deRotth A. Plastic repair of conjunctival defects with fetal membrane. *Arch Ophthalmol*. 1940;23:522–525.
2. Kim JC, Tseng SCG. Transplantation of preserved human amniotic membrane for surface reconstruction is severely damaged rabbit corneas. *Cornea*. 1995;14:473–484.
3. Jirsova K, Jones GLA. Amniotic membrane in ophthalmology: properties, preparation, storage and indications for grafting-a review. *Cell Tissue Bank*. 2017;18(2):193–204.
4. Ma KN, Thanos A, Chodosh J, Shah AS, Mantagos IS. A novel technique for amniotic membrane transplantation in patients with acute Stevens-Johnson syndrome. *Ocul Surf*. 2016;14(1):31–36.
5. Clare G, Bunce C, Tuft S. Amniotic membrane transplantation for acute ocular burns. *Cochrane Database Syst Rev*. 2022;9(9):CD009379.
6. Rahman I, Said DG, Maharajan VS, Dua HS. Amniotic membrane in ophthalmology: indications and limitations. *Eye (Lond)*. 2009;23(10):1954–1961.
7. Dunlap WA, Purnell WD, McPherson SD. Laboratory and clinical evaluation of a new synthetic

absorbable suture for ophthalmic surgery. *Adv Ophthalmol*. 1976;33:49–61.
8. Ramachandran C, Deshpande P, Ortega I, et al. Proof-of-concept study of electrospun PLGA membrane in the treatment of limbal stem cell deficiency. *BMJ Open Ophthalmol*. 2021;6(1): e000762.
9. Ramachandran C, Sangwan VS, Ortega I, et al. Synthetic biodegradable alternatives to the use of the amniotic membrane for corneal regeneration: assessment of local and systemic toxicity in rabbits. *Br J Ophthalmol*. 2019;103(2):286–292.
10. Uçakhan OO, Köklü G, Firat E. Nonpreserved human amniotic membrane transplantation in acute and chronic chemical eye injuries. *Cornea*. 2002;21(2):169–172.
11. Meller D, Pauklin M, Thomasen H, Westekemper H, Steuhl KP. Amniotic membrane transplantation in the human eye. *Dtsch Arztebl Int*. 2011;108(14):243–248.
12. Shah Z, Bakhshi SK, Bajwa MH, Khalil M, Dewan MC, Shamim SM. Human amniotic membrane as a dural substitute in neurosurgery: a systematic review. *Surg Neurol Int*. 2022;13:505.
13. Budenz DL, Barton K, Tseng SC. Amniotic membrane transplantation for repair of leaking glaucoma filtering blebs. *Am J Ophthalmol*. 2000;130:580–588.
14. Rauscher FM, Barton K, Budenz DL, Feuer WJ, Tseng SC. Long-term outcomes of amniotic membrane transplantation for repair of leaking glaucoma filtering blebs. *Am J Ophthalmol*. 2007;143:1052–1054.
15. Liu Y, Li H, Chen J. Shunt tube implantation combining amniotic membrane transplantation and implantation of Molteno implant for glaucoma after penetrating keratoplasty. *Yan Ke Xue Bao*. 2000;16:65–72.
16. Bourne GL. The microscopic anatomy of the human amnion and chorion. *Am J Obstet Gynecol*. 1960;79:1070–1073.
17. Dadkhah Tehrani F, Firouzeh A, Shabani I, Shabani A. A review on modifications of amniotic membrane for biomedical applications. *Front Bioeng Biotechnol*. 2021;8:606982.
18. Hopkinson A, McIntosh RS, Tighe PJ, James DK, Dua HS. Amniotic membrane for ocular surface reconstruction: donor variations and the effect of handling on TGF-beta content. *Invest Ophthalmol Vis Sci*. 2006;47:4316–4322.
19. Gicquel JJ, Dua HS, Brodie A, et al. Epidermal growth factor variations in amniotic membrane used for ex vivo tissue constructs. *Tissue Eng Part A*. 2009;15(8):1919–1927.
20. Fortunato SJ, Lombardi SJ, Menon R. Racial disparity in membrane response to infectious stimuli: a possible explanation for observed differences in the incidence of prematurity. Community Award Paper. *Am J Obstet Gynecol*. 2004;190(6):1557–1562; discussion 1562–1563.
21. López-Valladares MJ, Rodríguez-Ares MT, Touriño R, Gude F, Silva MT, Couceiro J. Donor age and gestational age influence on growth factor levels in human amniotic membrane. *Acta Ophthalmol*. 2010;88(6):e211–e216.
22. Smieja Z, Zakar T, Walton JC, Olson DM. Prostaglandin endoperoxide synthase kinetics in human amnion before and after labor at term and following preterm labor. *Placenta*. 1993;14(2):163–175.
23. Teixeira FJ, Zakar T, Hirst JJ, et al. Prostaglandin endoperoxide-H synthase (PGHS) activity and immunoreactive PGHS-1 and PGHS-2 levels in human amnion throughout gestation, at term, and during labor. *J Clin Endocrinol Metab*. 1994;78(6):1396–1402.
24. Tseng SC. Amniotic membrane transplantation for ocular surface reconstruction. *Biosci Rep*. 2001;21(4):481–489.
25. Paolin A, Trojan D, Leonardi A, et al. Cytokine expression and ultrastructural alterations in fresh-frozen, freeze-dried and c-irradiated human amniotic membranes. *Cell Tissue Bank*. 2016;17:399–406.
26. Hennerbichler S, Reichl B, Pleiner D, Gabriel C, Eibl J, Redl H. The influence of various storage conditions on cell viability in amniotic membrane. *Cell Tissue Bank*. 2007;8(1):1–8.
27. Tsai RJ, Li LM, Chen JK. Reconstruction of damaged corneas by transplantation of autologous limbal epithelial cells. *N Engl J Med*. 2000;343:86–93.
28. Koizumi N, Rigby H, Fullwood NJ, et al. Comparison of intact and denuded amniotic membrane as a substrate for cell-suspension culture of human limbal epithelial cells. *Graefes Arch Clin Exp Ophthalmol*. 2007;245(1):123–134.
29. Moriyama H, Kasashima Y, Kuwano A, Wada S. Anatomical location and culture of equine corneal epithelial stem cells. *Vet Ophthalmol*. 2014;17(2):106–112.
30. Schlötzer-Schrehardt U, Kruse FE. Identification and characterization of limbal stem cells. *Exp Eye Res*. 2005;81(3):247–264.
31. Papini S, Rosellini A, Nardi M, Giannarini C, Revoltella RP. Selective growth and expansion of human corneal epithelial basal stem cells in

a three-dimensional-organ culture. *Differentiation*. 2005;73(2-3):61–68.
32. Kimura K, Kawano S, Mori T, et al. Quantitative analysis of the effects of extracellular matrix proteins on membrane dynamics associated with corneal epithelial cell motility. *Invest Ophthalmol Vis Sci*. 2010;51(9):4492–4499.
33. Stevenson BR, Siliciano JD, Mooseker MS, Goodenough DA. Identification of ZO-1: a high molecular weight polypeptide associated with the tight junction (zonula occludens) in a variety of epithelia. *J Cell Biol*. 1986;103:755–766.
34. Stevenson BR. Understanding tight junction clinical physiology at the molecular level. *J Clin Invest*. 1999;104:3–4.
35. Wang Y, Chen M, Wolosin JM. ZO-1 in corneal epithelium; stratal distribution and synthesis induction by outer cell removal. *Exp Eye Res*. 1993;57:283–292.
36. Joseph A, Powell-Richards AO, Shanmuganathan VA, Dua HS. Epithelial cell characteristics of cultured human limbal explants. *Br J Ophthalmol*. 2004;88:393–398.
37. Lavker RM, Tseng SC, Sun T-T. Corneal epithelial stem cells at the limbus: looking at some old problems from a new angle. *Exp Eye Res*. 2004;78:433–446.
38. Martens JE, Arends J, Van der Linden PJ, De Boer BA, Helmerhorst TJ. Cytokeratin 17 and p63 are markers of the HPV target cell, the cervical stem cell. *Anticancer Res*. 2004;24:771–775.